

# Role of surface intermediates in the deactivation of Mg–Zr mixed oxides in acetone self-condensation: A combined DRIFT and ex situ characterization approach

Jorge Quesada<sup>a</sup>, Laura Faba<sup>a</sup>, Eva Díaz<sup>a</sup>, Simona Bennici<sup>b</sup>, Aline Auroux<sup>b</sup>, Salvador Ordóñez<sup>a,\*</sup>

<sup>a</sup> Department of Chemical and Environmental Technology, University of Oviedo (Faculty of Chemistry), Julián Clavería s/n., 33006 Oviedo, Spain

<sup>b</sup> Université Lyon 1, CNRS, UMR 5256, IRCELYON, Institut de Recherches sur la Catalyse et l'Environnement de Lyon, 2 Avenue Albert Einstein, F-69626, France

## ARTICLE INFO

### Article history:

Received 5 March 2015

Revised 15 April 2015

Accepted 17 April 2015

### Keywords:

DRIFT

Isophorones

Mesitylene

Mixed oxides

Base catalysis

## ABSTRACT

The role of the adsorbed reactants and intermediates on the performance and deactivation behavior of Mg–Zr mixed oxides as acetone self-condensation catalysts is studied in this work. DRIFT spectroscopy was used for identifying the adsorbed species and following their evolution during both acetone self-condensation reaction and thermo-desorption of pre-adsorbed reactants and products. The evolution of these species and the results of the characterization (nitrogen physisorption, temperature-programmed oxidation, and catalyst leaching) of catalysts samples taken in a continuous reactor at different temperatures (523, 623, and 723 K) and times on stream allow to determine that two concomitant deactivation causes are present in this reaction: the strong adsorption of dimers and trimers on the catalyst surface (especially important at the lowest temperature) and the formation of heavy condensation products physically deposited on the catalyst surface (more relevant at the highest temperature).

## 1. Introduction

There is an increasing interest in developing different processes for biomass upgrading in order to use this feedstock as petroleum substitutive. This replacement implies not only fuel manufacture, but also chemicals that are nowadays obtained from non-renewable resources [1]. In this framework, acetone plays a key role as platform molecule. This compound has two main renewable origins: acetone–butanol–ethanol fermentation processes [2], and the bio-oil obtained from biomass fast pyrolysis [3].

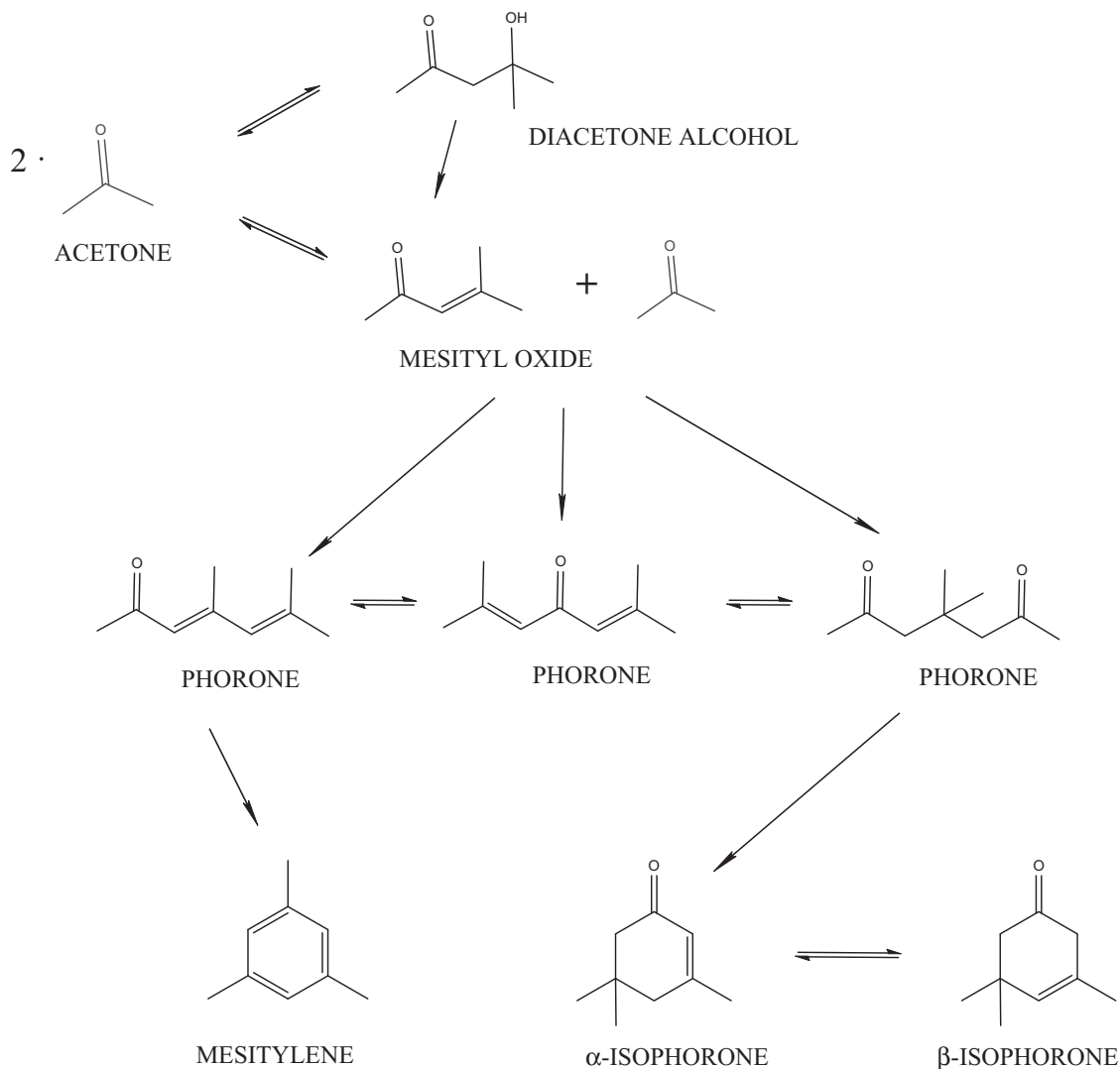
Considering the chemical structure of acetone, aldol condensation reactions are one of the most promising alternatives for obtaining different chemicals [4], such as diacetone alcohol, mesityl oxide, phorones, isophorones, or mesitylene. Although there are several references about the acetone self-condensation catalyzed by acid materials [5], this condensation is more usually catalyzed by basic sites. First studies developed this process in liquid phase, using homogeneous catalysts such as NaOH or KOH [6,7]. Nowadays, there are several reasons (environmental, technical, and economic) promoting the use of solid catalysts. Gas-phase acetone aldol self-condensation is a complex process, involving

different steps (aldol condensation, dehydrations, Michael condensations, and cyclations), and requiring different active sites in each one of these steps [8]. General reaction pathway is illustrated in Scheme 1. According to the most accepted mechanisms, good equilibrium between medium-strength basicity and weak acidity is needed to enhance the selectivity to cyclic trimers [8,9]. Different solid catalysts have been tested, obtaining good results with different alkaline-earth oxides [10,11], TiO<sub>2</sub> [12], and mixed oxides [5,13]. Mg–Zr mixed oxide is highlighted as one of the most appropriate catalysts, reaching a selectivity up to 50% for target products [8].

Deactivation is one of the most relevant and scarcely studied weaknesses of these solid catalysts, being commonly observed an important loss of activity in all the aldolization studies. Thus, more than 50% activity loses in less than 1 h of continuous reaction were observed using hydrotalcite-derived mixed oxides [14] and less than 15% of initial acetone conversion was detected in second cycles in batch configuration [15]. Deactivation affects both, overall reaction rates and product distributions, particularly at low time on stream [16]. Despite the relevance of this phenomenon, there is an important lack of information about the deactivation mechanisms in catalysis by basic sites. A deeper understanding of these mechanisms is needed for preventing catalyst deactivation, hence allowing the scaling-up of such processes. Previous works are not

\* Corresponding author.

E-mail address: [sordonez@uniovi.es](mailto:sordonez@uniovi.es) (S. Ordóñez).



**Scheme 1.** Simplified reaction mechanism of acetone self-condensation considering the insights obtained from DRIFT analyses.

very conclusive for determining the role of the different deactivation causes. Thus, there are references suggesting that the main deactivation cause is coke deposition [17–19], strong adsorption of water on the catalytic surface [20]; or morphological changes affecting strength distribution of the active sites [21].

More specific techniques are needed to get more accurate insights about catalyst deactivation in this reaction, needed for proposing strategies for stable operation and/or effective regeneration procedures. In this field, important information can be obtained by combining diffuse reflectance infrared fourier transform (DRIFT) spectroscopy with other characterization techniques, such as nitrogen physisorption and temperature-programmed oxidation (TPO). DRIFT spectroscopy allows analyzing the temporal evolution of surface functional groups and adsorbed intermediates at reaction conditions. Thus, DRIFT technique has been successfully applied to different deactivation studies, such as the study of stability and redox chemistry of Co(III) in aluminophosphate zeolites, catalyst deactivation in CO oxidation and shift reactions or butanal self-condensation over alkaline-earth mixed oxides [22–24].

The aim of this paper was to study the catalytic deactivation during the gas-phase acetone self-condensation. Considering the promising results obtained with MgZr mixed oxide, this material was chosen as model catalyst [8]. The effect of deactivation on measured selectivities and conversions was established by

combining DRIFT studies (temperature-programmed desorption of reactants and products, and continuous *in situ* reaction in the DRIFT chamber) with the characterization of catalyst samples aged at different temperatures and times on stream.

## 2. Experimental

### 2.1. Catalytic tests

Acetone self-condensation was studied using magnesia–zirconia mixed oxide as catalyst. Mg–Zr was synthesized using the sol–gel technique, obtaining a mixed oxide with a Mg/Zr ratio of 4.5 (result tested by ICP-MS). N<sub>2</sub> physisorption analyses corroborate its mesoporous character, with a surface area of 78 m<sup>2</sup>/g and a pore diameter of 34.2 nm. The synthesis method, as well as the characterization of this material, is deeply described in our previous work [26]. The evolution of the activity for acetone self-condensation was studied in a fixed bed reactor consisted of a 0.4 cm i.d. U-shaped quartz tube placed in a PID-controlled electric furnace. Catalyst samples (150 mg, 50–80  $\mu$ m particle diameter) were placed over a plug of quartz wool. Temperature is measured by a thermocouple placed inside the catalytic bed. Acetone is continuously fed with a syringe pump in a helium flow (3.2 vol.%), with a weight hour space velocity (WHSV) of 8 h<sup>-1</sup>.

These conditions were optimized in our previous work [8]. As it was previously demonstrated, mass transfer effects do not affect catalyst performance under these conditions [26]. Considering previous results, showing that product distribution markedly changes with temperature [8], stability analyses are carried out at 523 (larger selectivities for dimer formation), 623 (intermediate behavior), and 723 K (larger selectivities for trimer formation) for 8 h. During this time, reaction mixture is online analyzed by gas chromatography using a Shimadzu GC-2010 equipped with a FID detector. A CP-Sil 5 CB capillary column (15 m) is used as stationary phase. Peak assignment was performed using GC-mass spectra and responses were determined using standard calibration mixtures.

## 2.2. DRIFTS experiments

Diffuse reflectance infrared spectra were recorded in the 4000–1200  $\text{cm}^{-1}$  using a Thermo Electron Nicolet FTIR spectrometer equipped with a MCT/A detector. Instrument was calibrated with a resolution of 4  $\text{cm}^{-1}$ , collecting 256 scans/spectrum. The powder sample was placed inside a high temperature cell equipped with two ZnSe windows. 20 mg of catalysts was used in each experiment. Samples were heated *in situ* following the same procedure as in the reaction studies (1 h at 723 K in  $\text{N}_2$  flow). After this pre-treatment,  $\text{O}_2$  was removed and catalytic measurements were conducted under inert atmosphere ( $\text{N}_2$  flow of 20  $\text{mL min}^{-1}$ ). DRIFT spectra were recorded every 10 min and results are reported after subtraction of a reference spectrum of KBr (Fluka, >99%) and the corresponding background registered at the same temperature. Signals obtained were converted into Kubelka–Munk units. Temperature calibration allows referring all the results to the actual surface temperature. Calibration was repeated with nitrogen saturated in acetone and mesityl oxide, concluding that the flow composition has negligible influence on the sample temperature. This fact was in good agreement with the literature [27].

Two different types of DRIFT experiments were carried out, using this technique to identify and determine the stability of adsorption bands (TPD-DRIFT studies), as well as to perform catalytic activity studies, in order to compare the evolution with the time of adsorbed species concentration and gas-phase composition. Band assignment was done with standards and by comparison with data reported in the literature. A first adsorption at room temperature was carried out, saturating the catalytic surface with the probe molecule during 20 min. This saturation was conducted passing the  $\text{N}_2$  for a bubbler. After this time, this bubbler was bypassed and measurements were carried out with the pure inert gas, increasing the temperature of the cell. Concerning to the activity studies, analyses were carried out at the same temperature as the catalytic tests.

## 2.3. Characterization of spent catalysts

Considering the activity results, samples aged at fixed reaction conditions and recovered at different times on stream (1, 2, 4, 6, and 8 h) were taken for subsequent characterization in order to identify the deactivation causes. Changes in the morphology were estimated by nitrogen physisorption at 77 K in a Micromeritics ASAP 2020 surface area and porosity analyzer considering the BET approach. The irreversible adsorption of different products on the surface active sites was measured by lixiviation with organic solvents, being THF the most efficient solvent for these tests. The lixiviation was performed by immersing the catalyst in THF during 4 h in boiling THF in a flask equipped with a solvent condenser. Resulting liquid was analyzed by GC-MS using a Shimadzu QP-2010 with a 30-m long TRB-5MS capillary column as stationary phase. The presence of coke deposits was measured by TPO analysis on a Micromeritics TPD/TPR 2900 apparatus.

Aged catalysts (10 mg) were exposed to an oxygen stream (2.5%  $\text{O}_2$  in 20  $\text{mL min}^{-1}$  He flow) at increasing temperature (linear rate of 5  $\text{K min}^{-1}$  up to 800 K), being the combustion gases evolution monitored by mass spectroscopy.

## 3. Results

### 3.1. DRIFT analysis of the fresh catalyst

Absorption properties of the Mg–Zr mixed oxides were determined by DRIFT spectroscopy. Spectra were collected under inert conditions ( $\text{N}_2$  flow) at different temperatures (from 523 to 723 K). According to the literature [28], most of the chemically relevant information is obtained at the interval of 1200–2000  $\text{cm}^{-1}$ . Secondary and not-well defined signals were obtained at values above 3700  $\text{cm}^{-1}$ , being assigned to free OH groups [29]. These hydroxyl groups are considered inactive because they do not form hydrogen bonds, so they are not taken into account for this study. On the other hand, signal at 810–840  $\text{cm}^{-1}$  is also detected and identified as the Zr–O bond stretching mode [30]. This signal is not shown because its intensity is constant and it is not related to the active sites for the aldol condensation (acid–base pair sites mainly associated to MgO) [29]. DRIFT spectrum of the fresh catalyst is shown in Fig. 1. Main band is observed at 1433  $\text{cm}^{-1}$ , corresponding to the MgO stretching mode [29]. In addition to the MgZr phase identification; this analysis also allows identifying the surface basic sites of this material. Usually, the analysis of these sites requires the previous adsorption of an acid probe molecule. However, and in good agreement with studies already published by Aramendia and coworkers [29], the affinity between MgZr mixed oxide and  $\text{CO}_2$  is strong enough to saturate the surface with ambient  $\text{CO}_2$ , allowing the identification of different basic sites in terms of  $\text{CO}_2$  adsorption modes. DRIFT analyses are in good agreement with previous  $\text{CO}_2$ -TPD studies, identifying the different bands related to bicarbonate basic sites (located at 1232, 1480, and 1650–1700  $\text{cm}^{-1}$ ) [26,31] and those associated to bidentate basic sites (1325–1350  $\text{cm}^{-1}$ ) [29].

### 3.2. TPD-DRIFTS analysis of the adsorption of reactants and products

*In situ* DRIFT spectroscopy was used to identify the interactions among reaction intermediates and the catalyst surface. Before the TPD experiments, different chemicals involved in this reaction (acetone, diacetone alcohol, mesityl oxide, isophorones, and mesitylene) were adsorbed onto the catalyst surface at room temperature, by flowing an organic-saturated nitrogen flow. After this, gas flow was changed by pure  $\text{N}_2$  and temperature was raised to the set point. Results obtained reveal that all the compounds are rapidly adsorbed on the surface, reaching constant values after less

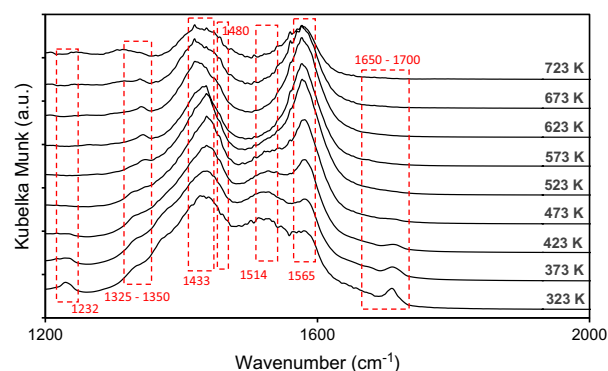


Fig. 1. DRIFT spectra of MgZr catalyst recorded at different temperatures.

than 10 min in the slowest case. This adsorption time was chosen to compare all the reported results. Fig. 2 shows the TPD-DRIFTS spectra of the catalyst saturated with different compounds, whereas the identification of each band is summarized in Table 1.

The high relevance of the  $\nu\text{C}=\text{O}$  interaction in the acetone spectra, as well as its splitting, indicates the relevance of surface enolates, key intermediates in the aldol condensation. The stability of acetone bands was corroborated in a separate experiment, saturating the catalyst with acetone and collecting spectra at increasing temperatures in flowing  $\text{N}_2$ , in order to analyze the desorption of this compound under inert conditions. Spectra obtained are shown in Fig. S1. There is not significant displacement of main bands, and the  $1738\text{ cm}^{-1}$  signal can be chosen to follow the acetone independently of the temperature. Besides, new bands observed at high temperature denote the acetone self-condensation, with bands of dimer and trimer products.

Spectrum obtained with the adsorption of mesityl oxide is more complicated, with more and stronger interactions. Detailed identification of the absorption bands is summarized in Table 1. Considering the intensity and the good resolution of band at  $1680\text{ cm}^{-1}$ , this signal is chosen to indicate the evolution of this compound. Same bands are also detected when diacetone alcohol is pre-adsorbed, but in much lower intensity. Desorption analysis of diacetone alcohol (Fig. S2) clearly demonstrates the instability of this intermediate, with a high relevance of  $-\text{OH}$  vibration modes ( $>3000\text{ cm}^{-1}$ ) produced by the dehydration of the diacetone alcohol to mesityl oxide. Taking into account the low intensity of main bands, as well as its negligible concentration observed during the reaction, this compound is not further considered in the DRIFT

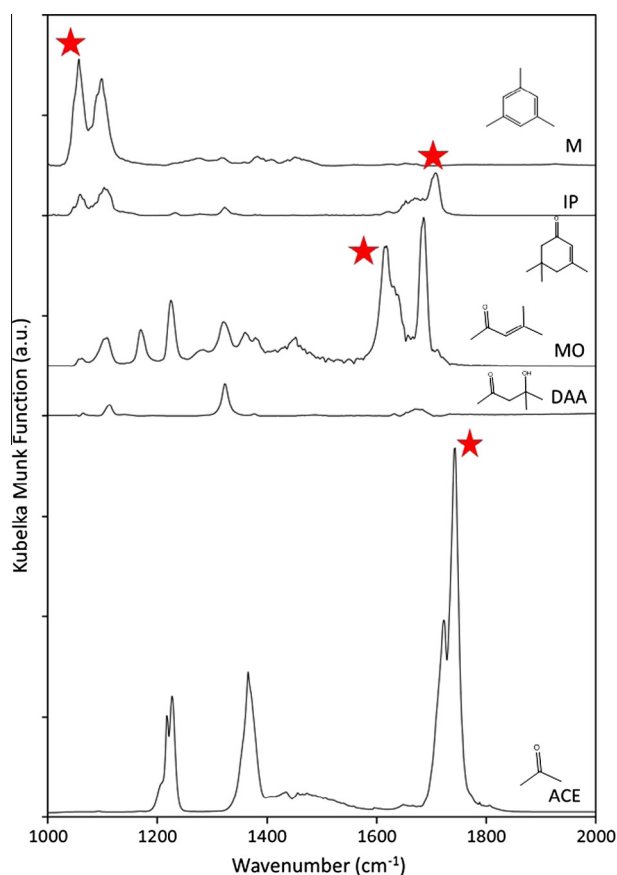


Fig. 2. TPD-DRIFTS spectra of different compounds involved in the acetone self-condensation. “★” indicates the bands selected for the identification of the adsorbed compounds. Nomenclature: ACE, acetone; DAA, diacetone alcohol; MO, mesityl oxide; IP, isophorone; M, mesitylene.

Table 1

Assignment of absorption frequencies of the reactants and products adsorbed on MgZr. Values obtained at 323 K after 10 min of adsorption.

| Molecule          | Vibration mode                                  | Frequency ( $\text{cm}^{-1}$ ) | Reference |
|-------------------|---|--------------------------------|-----------|
| Acetone           | $\nu\text{C}-\text{C}$                          | 1219                           | [32]      |
|                   | $\delta\text{C}-(\text{CH}_3)_2$                | 1365                           | [33]      |
|                   | $\nu\text{C}=\text{O}$                          | 1716–1738                      | [33,34]   |
| Diacetone alcohol | $\delta\text{CCH}$                              | 1066                           | [32]      |
|                   | Bending $\text{CH}_3-\text{CH}_2$               | 1115                           | [35]      |
|                   | $\delta\text{C}-(\text{CH}_3)_2$                | 1325–1381                      | [33]      |
|                   | $\nu\text{C}=\text{O}$ , $\nu\text{C}=\text{C}$ | 1649–1684                      | [33]      |
| Mesityl oxide     | Bending $\text{CH}_3-\text{CH}_2$               | 1111, 1170                     | [35]      |
|                   | $\nu\text{C}-\text{C}$                          | 1227                           | [32]      |
|                   | $\delta\text{C}-(\text{CH}_3)_2$                | 1325–1380                      | [33]      |
|                   | $\nu\text{C}=\text{O}$ , $\nu\text{C}=\text{C}$ | 1620–1686                      | [33]      |
|                   | $\nu\text{C}-\text{H}$                          | 2924–2978                      | [32,33]   |
| Isophorone        | $\delta\text{CCH}$                              | 1061                           | [32]      |
|                   | Bending $\text{CH}_3-\text{CH}_2$               | 1103                           | [35]      |
|                   | Bending $\text{C}=\text{O}$                     | 1236                           | [35]      |
|                   | $\delta\text{C}-(\text{CH}_3)_2$                | 1323                           | [33]      |
|                   | $\nu\text{C}=\text{O}$                          | 1674                           | [33]      |
|                   | $\nu\text{C}=\text{O}$                          | 1709                           | [32]      |
|                   | $\nu\text{C}-\text{H}$                          | 2883–2971                      | [32,33]   |
| Mesitylene        | $\delta\text{C}-\text{CH}_3$                    | 1023                           | [32]      |
|                   | Bending $\text{C}-\text{OH}$                    | 1280                           | [35]      |
|                   | $\delta\text{C}-(\text{CH}_3)_2$                | 1320                           | [33]      |
|                   | $\delta\text{C}-(\text{CH}_3)_2$                | 1385, 1458                     | [33]      |
|                   | $\nu\text{C}-\text{H}$                          | 2888–2971                      | [32,33]   |

analyses. The stretching  $\nu\text{C}=\text{O}$  mode of isophorones is considerably moved from the mesityl oxide one and it is located at  $1709\text{ cm}^{-1}$ . Considering this special feature, this band is used to analyze the evolution of this compound during the reaction. Finally, mesitylene main intensities are located at lower wavenumbers ( $<1100\text{ cm}^{-1}$ ), far from the wavenumbers more representative of other compounds. Taking into account the high intensity obtained at  $1023\text{ cm}^{-1}$  (corresponding to  $\delta\text{CCH}$ ) [32], this band is selected for following mesitylene evolution.

### 3.3. Studies of reaction mechanism by DRIFT spectroscopy

The evolution of previously reported bands with the temperature is very useful to corroborate the reaction mechanism. Spectra obtained are shown as supplementary information (Figs. S2–S5), whereas the evolution of the area of the characteristic bands selected for each compound is plotted in Figs. 3 and 4. Results observed in Fig. 3 are in good agreement with the hypothesis that trimers are only obtained from mesityl oxide, being the diacetone alcohol an unstable by-product. The instability of this compound (Fig. 3a) is corroborated by the high intensity of acetone at temperatures over 500 K, suggesting the decomposition of this molecule. At higher temperatures, the dehydration of this compound is also observed, yielding mesityl oxide. Same information is obtained analyzing the evolution of bands at 2979 and  $3365\text{ cm}^{-1}$  (Fig. 4), corresponding to H atom interactions and  $-\text{OH}$  interactions that reveal dehydration processes, respectively [29,32].

On the other hand, important signals of cyclic trimers are detected at temperatures higher than 400 K when mesityl oxide is fed (Fig. 3b), which evidences the reversibility of this process, since phorones are obtained from the reaction between mesityl oxide and acetone. Considering that acetone is not fed, this molecule can be only obtained by retro-aldolization (aldolization reverse reaction) of mesityl oxide. The presence of mesitylene even when the surface isophorone concentration is almost negligible suggests a direct cyclation of phorones into mesitylene. The highest intensity of isophorones, mainly at high temperatures, reveals

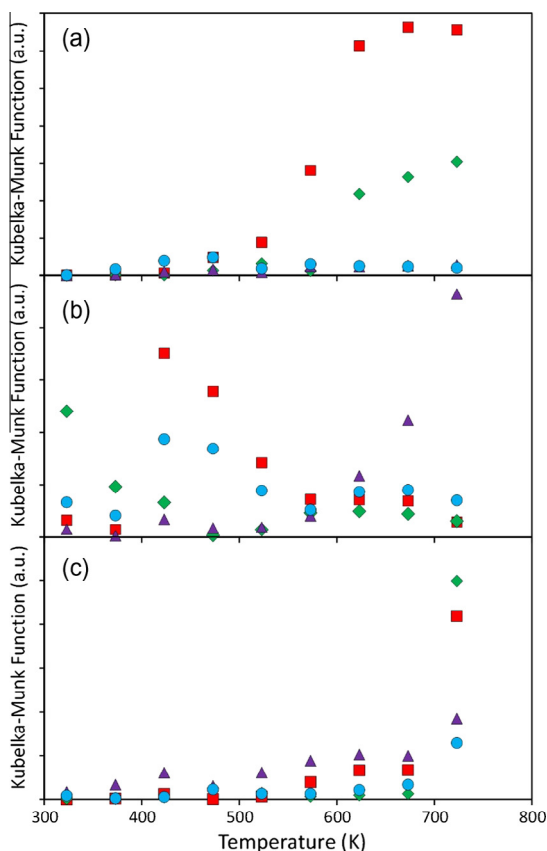


**Fig. 3.** Evolution of representative bands of the acetone self-condensation reactants and products when (a) diacetone alcohol; (b) mesityl oxide and (c) isophorones are pre-adsorbed. Symbols: (■) acetone; (◆) mesityl oxide; (▲) isophorone; and (●) mesitylene.

a strong interaction between these compounds and the catalyst surface. These results are congruent with Fig. 4b, where an increasing H<sub>2</sub>O signal evidences dehydration processes, needed to obtain cyclic trimers. Almost negligible acetone and mesityl oxide signals are observed when isophorone is fed (Fig. 3c), suggesting that the formation of isophorones is irreversible. This behavior is even more evident in the case of mesitylene, which has not reactivity because of the absence of any carbonyl group (constant spectrum). All the results observed with DRIFT spectroscopy allow modifying the previously proposed reaction mechanisms, considering the reversibility-irreversibility of each reaction step (Scheme 1).

One of the main causes of catalytic deactivation is the active sites blockage by coke deposition and DRIFT analyses are useful to determine the origin of these carbon deposits by identifying the presence of bands at 1590 cm<sup>-1</sup> in the TPD-DRIFT analyses of standard compounds, since these bands are attributed to highly conjugated polyaromatic structures [36]. Fig. 4c shows the evolution of this band with the temperature as function of the fed compound. Important signals of this band are obtained with all the tested compounds, especially with the trimers, suggesting that the coke formation in this reaction is an unspecific process that can be promoted by different adducts. The relevance of this process increases with the temperature, although it can be detected even at low temperatures when aromatic (mesitylene) or cyclic compounds (isophorones) are present.

#### 3.4. Reaction studies with continuous fed of acetone

Acetone aldol condensation has been performed in the DRIFT chamber at the same operation conditions as those used in the

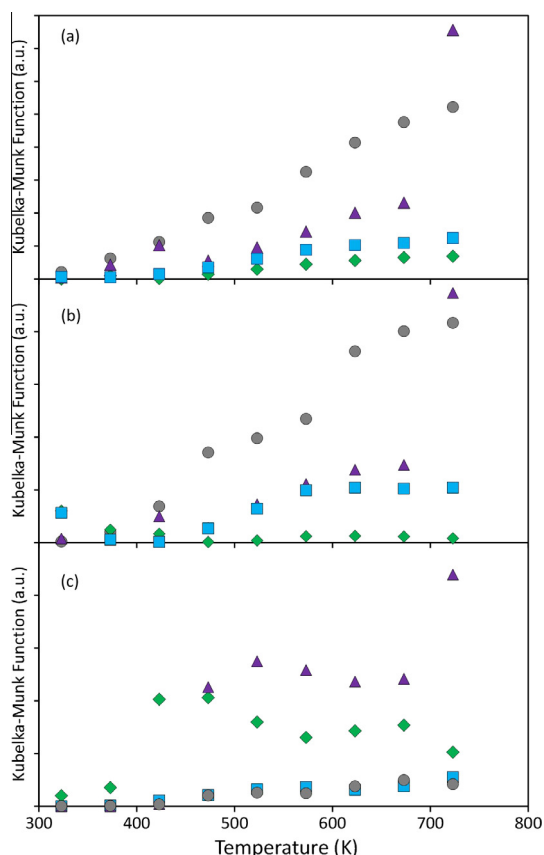


**Fig. 4.** Evolution of the peak intensity corresponding to (a) H atom ( $\nu\text{C-H}$ , 2979 cm<sup>-1</sup>); (b) H<sub>2</sub>O (3365 cm<sup>-1</sup>); and (c) highly conjugated polyaromatic structures (1590 cm<sup>-1</sup>) with time as function of the compound fed. Symbols: (●) diacetone alcohol; (◆) mesityl oxide; (▲) isophorone; and (■) mesitylene.

fixed bed reactor, in which outlet gases were analyzed by GC-FID. Consequently, data obtained by two methodologies are comparable. DRIFT spectra are shown in Fig. S6. Considering the intensity of bands previously identified, results are analyzed in Fig. 5. As it could be expected, there is a continuous decrease in the acetone signals (Fig. 5a), more noticeable at temperatures higher than 473 K. These results are congruent with the evolution of the acetone conversion calculated from the gas-phase compositions. Concerning to the products evolution (Fig. 5b), it must be highlighted that bands related to isophorones are observed even at the lowest temperature. Same behavior is observed with the mesitylene but with lower intensity. Thus, trimers are present even at low temperature, in contrast to previously reported results [8]. The interaction between trimer compounds and the catalytic surface is so strong that higher temperatures are needed to desorb them from the catalyst surface.

It is interesting to note that the isophorone initial adsorption seen by DRIFT is simultaneous to the initial loss in the carbon balance closure (<80%) measured in the gas phase by GC. Adsorption of reaction intermediates decreases as the temperature increases, in such a way that only phorones signal is clearly detected at 723 K, whereas cyclic trimers are more visible in the gas phase. On the other hand, there was an increase in signals from 2900 to 3600 cm<sup>-1</sup> at increasing temperatures (Fig. S6). These increases are assigned to free water and H interactions obtained during cyclization processes [29]. In the same way, as the temperature increases, more intense signals attributed to polyaromatic structures are detected (1590 cm<sup>-1</sup>), suggesting the cracking of oxygenated compounds yielding coke precursors [25]. These results corroborate the decrease in the carbon balance observed

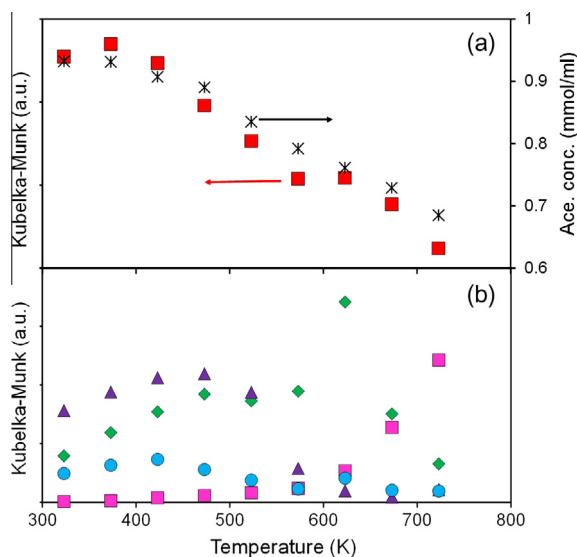


**Fig. 5.** (a) Evolution with the temperature of representative peak intensity of adsorbed acetone when acetone is continuously fed to the DRIFT chamber, compared to acetone concentration at the outlet of a fixed bed reactor; (b) evolution with the temperature of the intensity of the representative peaks of the following reaction products: (■) acetone; (◆) mesityl oxide; (■) phorones; (▲) isophorone; (●) and mesitylene.

in gas-phase analyses. In conclusion, the breakup curve obtained by DRIFT suggests three different processes leading to catalytic deactivation: strong adsorption of several reaction intermediates, the presence of water, and the formation of unreactive

carbonaceous species. These processes have been individually identified as deactivation causes in different condensations [17,18–21], so their individual role in this condensation must be deeper analyzed.

### 3.5. Deactivation studies

Deactivation studies were carried out at three temperatures (523, 623, and 723 K), studying the evolution of different compounds in the gas phase as well as the interactions with the catalytic surface. These temperatures were chosen considering the different activity results observed in the previous experiments studying the influence of the temperature on catalyst performance (Fig. 3). The lowest temperature corresponds to the highest selectivity for dimers formation, whereas the highest corresponds to almost total conversion and high selectivity for trimer formation, and the other one shows an intermediate behavior. Results obtained in the fixed bed reactor are compared with those obtained by DRIFT at similar operation conditions, considering the bands related to the different adducts as well as the evolution of bands located at  $1590\text{ cm}^{-1}$  and  $>3000\text{ cm}^{-1}$ , assigned to  $\text{CO}_2$  and free water, respectively [25,30].

Fig. 6a and b compare results obtained in the gas-phase analyses with the evolution of the DRIFT spectra at 523 K for 8 h, reproducing same conditions as in reactions in U-tube reactor. Acetone conversion, product selectivities, and carbon balance in the gas phase are calculated as in previous works [8]. There is a constant and slight decrease in the acetone conversion observed by GC-FID, mainly during the first two hours on stream. After 6 h, the acetone conversion decreases from 34% to 22% (a loss of

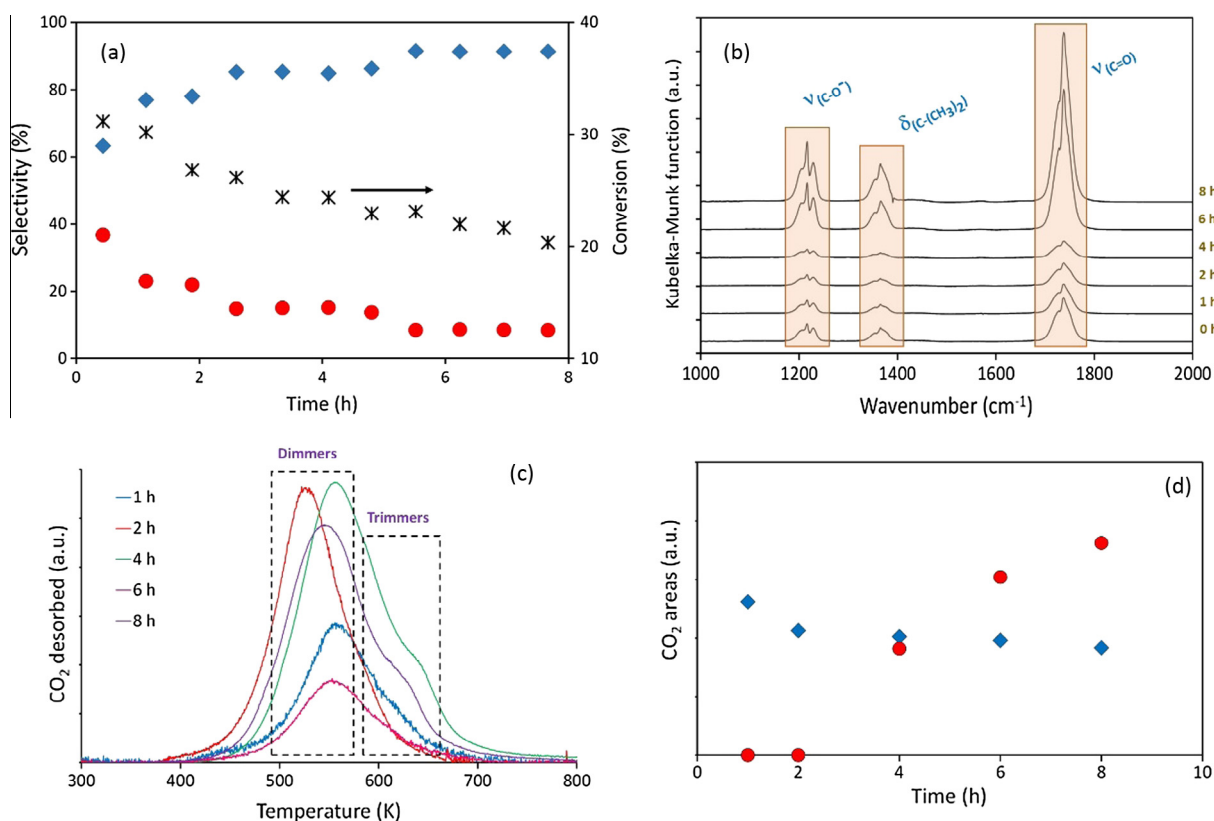


**Fig. 6.** Evolution of the activity of MgZr with time at 523 K considering: (a) the gas phase; (b) the catalytic surface; (c) TPO profiles of spent catalyst; and (d) analyses of  $\text{CO}_2$  areas obtained by TPO normalized as function of the higher value obtained. Symbols: (×) acetone conversion; (◆) dimers; and (●) trimers.

activity of 35%). The carbon balance keeps almost constant, with a slight decrease from 82% to 79% after these six hours on stream. These results discard a relevant influence of coke formation, process leading to more markedly decreases of carbon balance.

The evolution of the selectivities is shown by families (Fig. 6a); dimers (diacetone alcohol and mesityl oxide), and trimers (phorones, isophorones, and mesitylene). After 6 h of reaction, the selectivity of C9's is lower than 9%, with an increase in the C6's adducts higher than 40%. Considering each compound individually, the selectivity of phorones increases, whereas the selectivity of isophorones and mesitylene is almost negligible after four hours on stream. These behaviors can be justified observing the DRIFT spectra. Three main bands are identified, corresponding to  $\nu(\text{C}-\text{O}^-)$ ,  $\delta(\text{C}-(\text{CH}_3)_2)$ , and  $\nu(\text{C}=\text{O})$ , respectively. These bands are common to almost all the compounds involved in this reaction but the displacement of the wavenumber is related with the chemical transformation taking place. The highest intensity corresponds to  $\nu(\text{C}=\text{O})$ , around  $1740\text{ cm}^{-1}$ , and, according to the literature, it is attributed to linear phorones [13]. The other two bands correspond to of acetone and mesityl oxide.

These results suggest that the presence of two oxygen atoms in linear phorones increases the strength of adsorption of these molecules with  $\text{Mg}^{2+}$  ions. The marked increase in the intensity of this band up to 2 h corresponds to the maximum decrease in the activity observed in the gas phase. The strong adsorption of linear trimers justifies the decrease in C9 selectivity detected in the gas phase. Bands related to free  $\text{H}_2\text{O}$  are only detected during the first hour, indicating that the cyclation of phorones is suppressed after this time. Besides, considering the reversibility of this reaction [9,12], the permanent adsorption induces the decomposition of these phorones into dimers, which justifies the decrease of trimers selectivity. In good agreement with the absence of coke formation, no signals at  $1590\text{ cm}^{-1}$  were observed, neither during the first 8 h nor after longer times on stream. DRIFT analyses were carried on for 24 h (Fig. S7), without observing significant differences.

DRIFT results are congruent with the analyses of the spent catalysts. The amount of permanently adsorbed molecules as well as their strength of this adsorption is measured by TPO. In order to identify the peaks obtained, the oxidation of each product is studied individually, saturating 10 mg of fresh catalyst with each compound at 293 K for 30 min and studying the evolution of CO and  $\text{CO}_2$  signals as function of the temperature under oxygen flow (temperature rate of  $5\text{ K min}^{-1}$ ) (Fig. S8). Differences on the combustion behavior of the considered compounds of each family are so slight that a good individual identification is not possible. However, results can be analyzed by families. The total oxidation of the dimers occurs in a range of 520–570 K, whereas the oxidation of the trimers occurs in two steps, the first one overlapped with dimers combustion, but the second one takes place at temperatures from 600 to 650 K. TPO profiles obtained with the spent catalysts can be observed in Fig. 6c and d. No combustion temperatures higher than 573 K are observed in profiles obtained after less than four hours, indicating a majority adsorption of dimers and acetone. After this time, a secondary peak close to 623 K reveals the presence of heavier compounds. Considering that there are not cyclic compounds neither in the gas phase nor on the catalytic surface, this peak is attributed to phorones. Concerning to the areas, there is an important increase during the first two hours, indicating an important adsorption that is holding after this time, in good agreement with the DRIFT profiles. GC–MS analyses after lixiviation with THF are also congruent with these results (Table 2), being phorones and, with lower intensity, isophorones, the only detected compounds. The evolution of morphological parameters is also shown in Table 2. According to these results, no significant changes on the surface area are observed during these 8 h.

**Table 2**

Summary of surface areas and lixiviation tests for the catalysts used for aldol condensation reactions at different temperatures and times on stream. Lixiviation results are normalized using the lowest value obtained (phorones at 523 K after 2 h) as reference.

| T (K) |  |         | Time (h) |       |       |       |      |
|-------|--|---------|----------|-------|-------|-------|------|
|       |  |         | 1        | 2     | 4     | 6     | 8    |
| 523   | Lixiviation                            | MO      | –        | –     | –     | –     | –    |
|       |  | IP      | 1.1      | 1.0   | –     | –     | –    |
|       |  | M       | –        | –     | –     | –     | –    |
|       |  | F       | 3.3      | 4.9   | –     | –     | –    |
|       |  | Heavies | 4.5      | 3.2   | 6.3   | 9.5   | 8.6  |
|       | Surface area ( $\text{m}^2/\text{g}$ ) | 96.7    | 50.7     | 103.2 | 66.0  | 65.1  |      |
| 623   | Lixiviation                            | MO      | –        | –     | –     | –     | –    |
|       |  | IP      | –        | 7.0   | 70.0  | 63.3  | 10.0 |
|       |  | M       | –        | –     | –     | –     | –    |
|       |  | F       | –        | 1.1   | 11.7  | 13.5  | 1.2  |
|       |  | Heavies | 24.8     | 39.9  | 137.5 | 116.7 | 62.1 |
|       | Surface area ( $\text{m}^2/\text{g}$ ) | 80.9    | 74.0     | 73.8  | 81.6  | 88.1  |      |
| 723   | Lixiviation                            | MO      | –        | –     | –     | –     | –    |
|       |  | IP      | 10.7     | –     | 147.2 | 22.0  | 26.6 |
|       |  | M       | –        | –     | 129.3 | –     | –    |
|       |  | F       | –        | –     | 16.0  | 2.4   | 2.1  |
|       |  | Heavies | 25.0     | 30.3  | 34.4  | 59.0  | 85.8 |
|       | Surface area ( $\text{m}^2/\text{g}$ ) | 87.6    | 87.0     | 90.8  | 98.6  | 93.3  |      |

All the analyses are congruent with the hypothesis that the strong adsorption of phorones and isophorones, with a partial blockage of the active sites, is the main cause of deactivation at 523 K. This adsorption reaches its maximum in 2 h and, after this period, there is a stable state with relevant conversion. Consequently, this effect can be considered more as an inhibitory effect than a deactivation process, suggesting that it could be possible to work at high dimer yields just working with highest catalyst loadings.

Same procedure was followed performing the reaction at higher temperature (623 K). Fig. 7a and b compare results obtained in the gas-phase analyses with the evolution of the DRIFT spectra at 623 K. After 8 h on stream, conversion decreases about 50% (from 34% to 18%), thus the relevance of deactivation increases. Carbon balance only decreases from 86% to 83%. However, product distributions in both experiments (523 and 623 K) are very different. In this last case (623 K), selectivities reach almost stable values after the fourth hour (75% for dimers and 25% for trimers). These results are congruent with spectra obtained by DRIFT spectroscopy. Bands related to  $\nu\text{C}=\text{O}$  isophorones vibration modes ( $1620\text{--}1700\text{ cm}^{-1}$ ) and  $\delta\text{CH}_2$  of mesitylene ( $1440\text{--}1460\text{ cm}^{-1}$ ) are presented since the earliest times on stream. Their intensities are almost constant during the 8 h, indicating that the adsorption of these compounds is not the main cause of the deactivation. Signals related to the adsorption of enolate groups have an important increase as the reaction time increases, corresponding to the wavenumbers of different trimer adsorptions. This strong adsorption and the subsequent oligomerization can explain the evolution of product selectivities. In good agreement, signals of poly-aromatic structures (coke precursors) are obtained after 6 h, being much more important after 12 h of reaction (see DRIFT of 24 h in Fig. S9), indicating that this temperature is high enough to polymerize the trimers.

The evolution of lixiviation analyses agrees with the stability studies and permanent adsorption of isophorones and phorones (Table 2). The important decrease in the intensity of these compounds corresponds to the appearance of coke signals in DRIFT analyses. In good agreement, new peaks were detected by GC–MS after catalyst leaching in THF. These peaks were not identified but their molecular mass (258 and multiples of that) are congruent with the partial decomposition of different

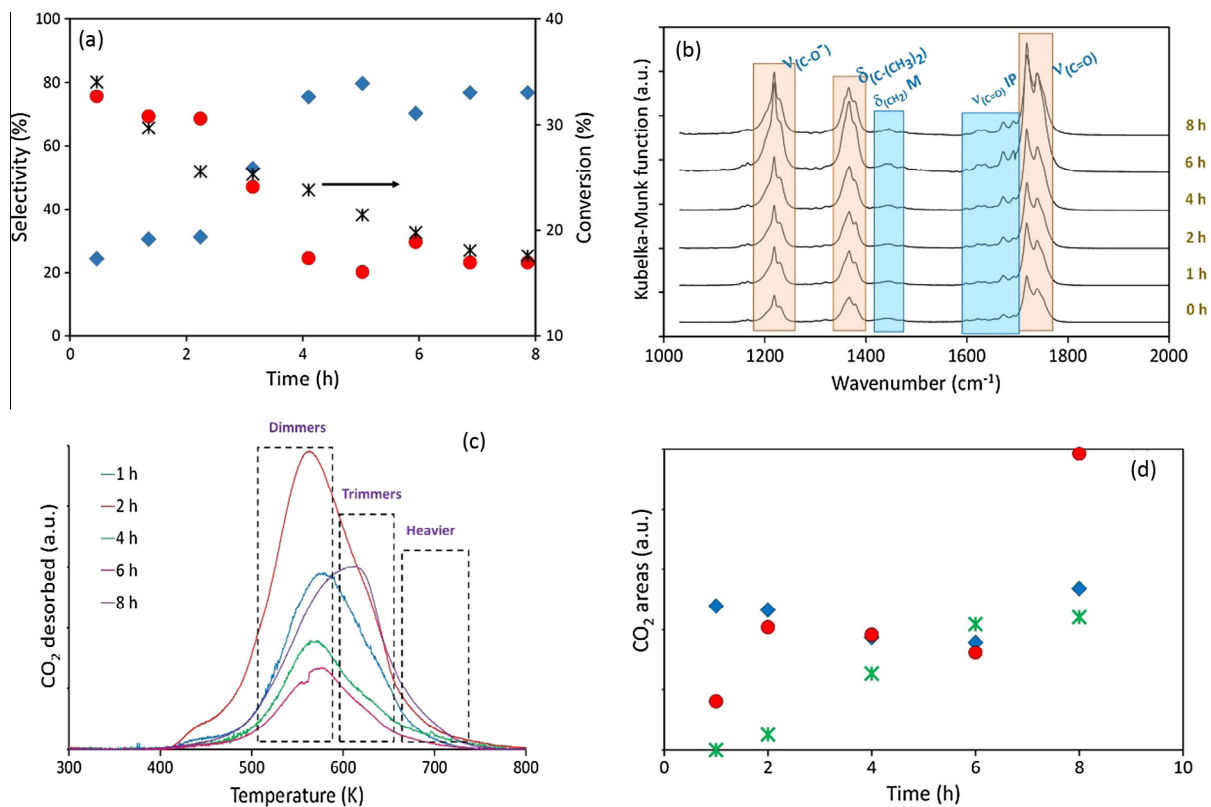


**Fig. 7.** Evolution of the activity of MgZr with time at 623 K considering: (a) the gas phase; (b) the catalytic surface; (c) TPO profiles of spent catalyst; and (d) analyses of CO<sub>2</sub> areas obtained by TPO normalized as function of the higher value obtained. Symbols: (×) acetone conversion; (◆) dimers; (●) trimers; (✱) and heavy compounds.

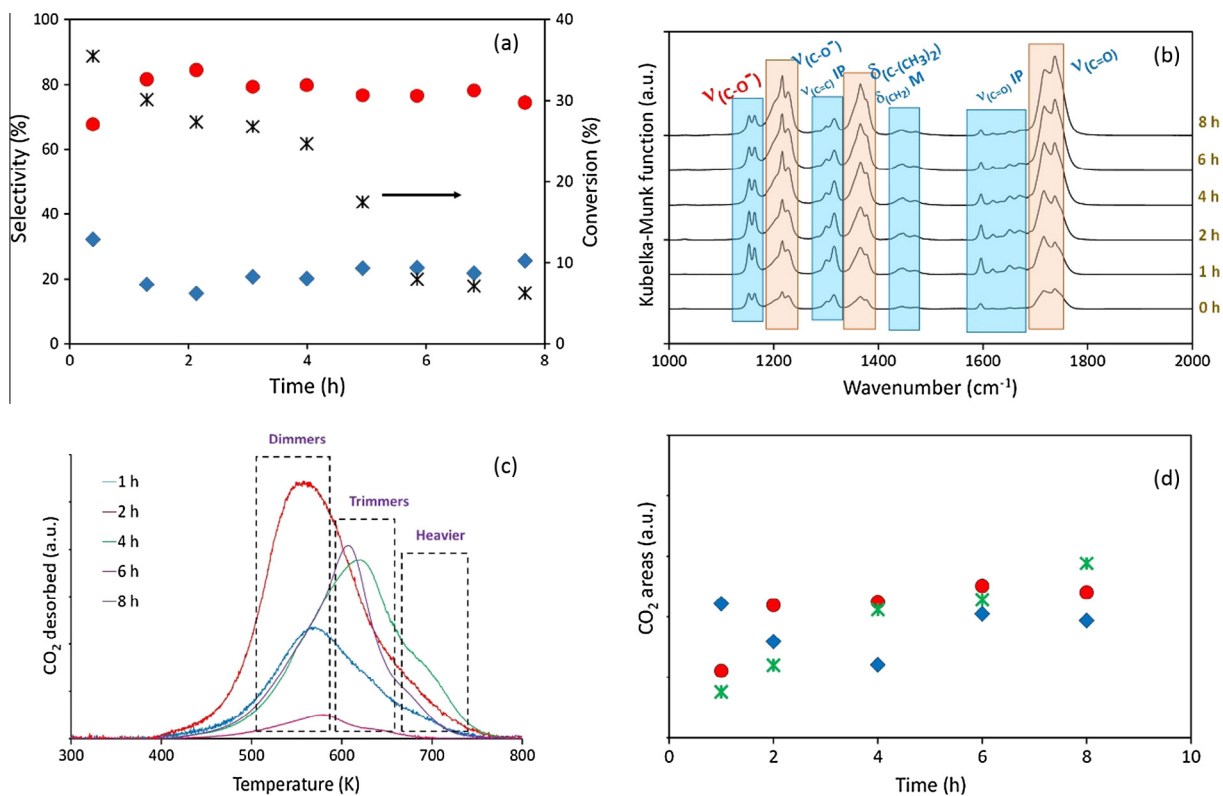


**Fig. 8.** Evolution of the activity of MgZr with time at 723 K considering: (a) the gas phase; (b) the catalytic surface; (c) TPO profiles of spent catalyst; and (d) analyses of CO<sub>2</sub> areas obtained by TPO normalized as function of the higher value obtained. Symbols: (×) acetone conversion; (◆) dimers; (●) trimers; (✱) and heavy compounds.

oligomers. These side reactions are favored by the stability of the isophorone adsorption, producing heavier condensation products and fouling the catalytic surface. This hypothesis was corroborated by TPO analyses, as it is shown in Fig. 7c and d. The presence of heavy compounds is demonstrated by the displacement of oxidation peaks to higher temperatures, and the presence of peaks with maximum over 700 K. This behavior was previously observed in studies of deactivation on MgO materials [17]. Considering the mesoporous character of MgZr and the irregular surface of the coke, its formation can produce an increase in the surface area and an important decrease in the pore diameter. The increase in the surface area after the first four hours is also in good agreement with this hypothesis. This phenomenon was previously observed in other processes involving polymerization of reaction products [37].

Finally, results at 723 K are summarized in Fig. 8. The loss of activity observed in gas phase is much marked at this temperature. During the first four hours, there is a soft decrease in the acetone conversion. This deactivation is much more important during the next two hours, with a decrease of almost 70% in the activity. After the sixth hour, the acetone conversion keeps constant in 8%, whereas the C9/C6 ratio was almost the same during all the period. These results correspond to a final carbon balance of 51%, a decrease of almost 30% respect to the initial value. Concerning to the DRIFT spectra, those bands related to the main compounds keep almost constant during all the period, but it must be highlighted the appearance of new bands related to isophorones and mesitylene as well as with a displacement from the theoretical values of these compounds. These displacements can be justified by the formation of oligomers that have similar interactions with the catalytic surface but more complex chemical structures.

The presence of carbonaceous deposits is evidenced by the TPO analyses (Fig. 8c and d): the intensity of the peaks at the highest temperature increases with time. The lower concentration of trimers observed by lixiviation analyses is congruent with their transformation into heavier compounds. Despite increasing trend of heavier compounds area, this increase is not enough to explain the stability results. This effect can be justified by the formation of coke deposits and not only oligomers. These compounds are so stable than they cannot be successfully removed from the catalytic surface, causing a permanent deactivation. This permanent loss of activity was confirmed by DRIFT analyses up to 24 h. As it can be observed in Fig. S10, the acetone conversion is negligible at longer times. The surface of spent catalysts is black from the first two hours, in contrast to spent catalysts used at lower temperatures, due to the presence of coke. Likewise, higher signals are obtained in lixiviation analyses (Table 2), mainly those referred to heavier compounds. Thus, MgZr in the acetone self-condensation at 723 K suffers a strong deactivation caused by the coke deposition, and the catalyst regeneration must be accomplished by the burning of these carbonaceous deposits to try to recover its initial activity.

The trend observed for the selectivities (which remain mostly constant during the experiment) suggests that solid carbonaceous deposits physically block the active sites, avoiding interaction with the active sites, which modifies products distribution. By contrast, at the other two temperatures, the interaction of the adsorbed molecules with the active sites tunes the behavior of the active sites leading to variation in the selectivity with the time on stream.

#### 4. Conclusions

The catalytic stability during acetone gas-phase self-condensation has been studied by different and complementary techniques. Results obtained indicate that deactivation causes depend on the operation temperature. At low temperature, no

oligomers were detected. The deactivation is due to the stable adsorption of dimers and trimers, mainly affecting to the C9/C6 ratio. At medium temperatures, first carbonaceous deposits were detected, identified as side products of phorones oligomerization. At high temperature, the deactivation is stronger and permanent, due to the formation of coke deposits on the surface of the active sites.

#### Acknowledgments

This work was supported by the Spanish and Asturian Governments (Contracts CTQ2011-29272-C04-02 and FC-15-GRUPIN14-078). J. Quesada thanks the Government of the Principality of Asturias for a Ph.D. fellowship (Severo Ochoa Program).

#### Appendix A. Supplementary material

Supplementary data associated with this article can be found, in the online version, at <http://dx.doi.org/10.1016/j.jcat.2015.04.029>.

#### References

- [1] H. Kayser, C.R. Müller, C.A. García-González, I. Smirnova, W. Leitner, P. Domínguez de María, *Appl. Catal. A* 445–446 (2012) 180.
- [2] P. Patakova, M. Linhova, M. Rychtera, L. Paulova, K. Melzoch, *Biotechnol. Adv.* 31 (2013) 58.
- [3] D. Manusr, T. Yoshikawa, K. Norinaga, J. Hayashi, T. Tago, T. Masuda, *Fuel* 103 (2013) 130.
- [4] W. Yin, R.H. Venderbosch, G. Bottari, K.K. Krawczyk, K. Barta, H.J. Heeres, *Appl. Catal. B* 166 (2015) 56.
- [5] G.S. Salvapati, K.V. Ramanamurthy, M. Janardanarao, *J. Mol. Catal.* 54 (1989) 9.
- [6] K.K. Rao, M. Gravelle, J. Sanchez Valente, F. Figueras, *J. Catal.* 173 (1998) 115.
- [7] R.T. Morrison, R.N. Boyd, *Organic Chemistry*, Allyn and Bacon Inc., Boston, 1987. p. 898.
- [8] L. Faba, E. Díaz, S. Ordóñez, *Appl. Catal. B* 142–143 (2013) 387.
- [9] J.I. Di Cosimo, V.K. Díez, C.R. Apesteguía, *Appl. Catal. A* 137 (1996) 149.
- [10] M.G. Álvarez, A.M. Frey, J.H. Bitter, A.M. Segarra, K.P. de Jong, F. Medina, *Appl. Catal. B* 134 (2013) 231.
- [11] I. Krivstov, L. Faba, E. Díaz, S. Ordóñez, V. Avdin, S. Khainakov, J.R. García, *Appl. Catal. A* 477 (2014) 26.
- [12] P. Kústrowski, D. Sulkowska, L. Chmielarz, A. Rafalska-Lasocha, B. Dudek, R. Dziembaj, *Microporous Mesoporous Mater.* 78 (2005) 11.
- [13] M. Zamora, T. López, M. Asomoza, R. Meléndrez, R. Gómez, *Catal. Today* 116 (2005) 234.
- [14] S. Abelló, D. Vijaya-Shankar, J. Pérez-Ramírez, *Appl. Catal. A* 342 (2008) 119.
- [15] F. Winter, V. Koot, A. Jos van Dillen, J.W. Geus, K.P. de Jong, *J. Catal.* 236 (2005) 91.
- [16] J.E. Rekoske, M.A. Barteau, *Ind. Eng. Chem.* 50 (2011) 41.
- [17] J. Di Cosimo, C.R. Apesteguía, *J. Mol. Catal.* 130 (1998) 177.
- [18] V.K. Díez, C.R. Apesteguía, J.I. Di Cosimo, *Stud. Surf. Sci. Catal.* 139 (2001) 303.
- [19] Y. Sugi, T. Matsuzaki, T. Hanaoka, K. Takeuchi, T. Tokoro, G. Takeuchi, *Stud. Surf. Sci. Catal.* 60 (1991) 303.
- [20] S. Talwalkar, S. Mahajani, *Appl. Catal. A* 302 (2006) 140.
- [21] F. Prinetto, D. Tichit, R. Teissier, B. Coq, *Catal. Today* 55 (2000) 103.
- [22] L.E. Iton, I. Choi, J.A. Desjardins, V.A. Maroni, *Zeolites* 9 (1989) 535.
- [23] C.S. Polster, H. Nair, C.D. Baertsch, *J. Catal.* 266 (2009) 308.
- [24] E. Río, S.E. Collins, A.I. Aguirre, X. Chen, J.J. Delgado, J.J. Calvino, S. Bernal, *J. Catal.* 316 (2004) 210.
- [25] W. Shen, G.A. Tompsett, R. Xing, W.C. Conner, G.W. Huber, *J. Catal.* 286 (2012) 248.
- [26] L. Faba, E. Díaz, S. Ordóñez, *Appl. Catal. B* 113–114 (2012) 201.
- [27] H.G. Li, M. Rivallan, F. Thibault-Starzyk, A. Travert, F.C. Meunier, *Phys. Chem. Chem. Phys.* 15 (2013) 7321.
- [28] J.T. Kozlowski, M.T. Aronson, R.J. Davis, *Appl. Catal. B* 96 (2010) 508.
- [29] M.A. Aramendía, V. Boráu, C. Jiménez, A. Marinas, J.M. Marinas, J.A. Navío, J.R. Ruiz, F.J. Urbano, *Colloid Surf. A* 234 (2004) 17.
- [30] N.R.E. Radwan, *Appl. Catal. A* 299 (2006) 103.
- [31] V.K. Díez, C.R. Apesteguía, J.I. Di Cosimo, *Catal. Today* 63 (2000) 53.
- [32] W.F. Wang, A. Stevenson, D.C. Reuter, J.M. Sirota, *Spectrochim. Acta A* 57 (2001) 1603.
- [33] C. Drouilly, J.M. Krafft, F. Averseng, H. Lauron-Pernot, D. Bazer-Bachi, C. Chizallet, V. Lecocq, G. Costentin, *Catal. Today* 205 (2013) 67.
- [34] N.E. Fouad, P. Thomasson, H. Knözinger, *Appl. Catal. A* 194 (2000) 213.
- [35] J. Gao, A.V. Teplyakov, *J. Catal.* 319 (2014) 136.
- [36] K. Matsushita, A. Hauser, A. Marafi, R. Koide, A. Stanislaus, *Fuel* 83 (2004) 1031.
- [37] V. Zarubina, C. Derlof, B. Van der Linden, F. Kapteijn, H.J. Heeres, M. Makkee, I. Melian-Cabrera, *J. Mol. Catal. A* 381 (2014) 179.